Aalto University

OPEN ACCESS

This is an electronic reprint of the original article.
This reprint may differ from the original in pagination and typographic detail.

Prabakaran, K.; Jayasakthi, M.; Surender, S.; Pradeep, S.; Sanjay, S.; Ramesh, Raju; Balaji, M.; Baskar, K.

Influence of InGaN interlayer thickness on GaN layers grown by metal organic chemical vapour deposition

Published in:
APPLIED PHYSICS A-MATERIALS SCIENCE AND PROCESSING

DOI:
10.1007/s00339-019-2503-2

Published: 01/03/2019

Document Version
Peer-reviewed accepted author manuscript, also known as Final accepted manuscript or Post-print

Please cite the original version:
Prabakaran, K., Jayasakthi, M., Surender, S., Pradeep, S., Sanjay, S., Ramesh, R., Balaji, M., & Baskar, K. (2019). Influence of InGaN interlayer thickness on GaN layers grown by metal organic chemical vapour deposition. *APPLIED PHYSICS A-MATERIALS SCIENCE AND PROCESSING*, *125*(3), Article 206. https://doi.org/10.1007/s00339-019-2503-2

This material is protected by copyright and other intellectual property rights, and duplication or sale of all or part of any of the repository collections is not permitted, except that material may be duplicated by you for your research use or educational purposes in electronic or print form. You must obtain permission for any other use. Electronic or print copies may not be offered, whether for sale or otherwise to anyone who is not an authorised user.

Influence of InGaN Interlayer thickness on GaN layers grown by Metal Organic Chemical Vapour Deposition

K.Prabakaran[1*], M. Jayasakthi[1], S.Surender[1], S. Pradeep[1], S. Sanjay[1], R. Ramesh[3], M. Balaji[4], K. Baskar[1, 2*]

[1] Crystal Growth Centre, Anna University, Chennai, India

[2] Manonmaniam Sundaranar University, Tirunelveli, India

[3] Department of Electronics and Nanoengineering, Aalto University, Finland

[4] Department of Energy, University of Madras, Guindy Campus, Chennai, India

Abstract:

InGaN interlayer was grown between GaN layers on sapphire substrate using metal organic chemical vapour deposition. The crystalline quality of the sample was investigated using high-resolution X-ray diffraction. The Indium composition and InGaN thickness were determined to be 10-15% and 5-10 nm respectively. Transmission electron microscopy image revealed the interfacial characteristics of InGaN and GaN layers. Raman spectroscopy revealed prominent GaN peak positions with InGaN shoulder peaks. The growth mode of InGaN and GaN were determined as nanoislands with helical-like morphology by atomic force microscopy. Hall measurement showcased improvement in the mobility and bulk concentration for the GaN/InGaN (5nm)/GaN structures.

Keywords: InGaN, High-Resolution X-ray Diffraction, Transmission Electron Microscopy, Hall Measurement

***Corresponding Author**

Dr. K. Prabakaran
Crystal Growth Centre
Anna University
Chennai-25, India
E-Mail: karanphy07@gmail.com (K. Prabakaran)
drbaskar2009@gmail.com (K. Baskar)

1. Introduction

GaN and related III-nitride alloy materials attract considerable interest in the development of optoelectronics, high-power and high-frequency electronic applications **[1-3].** However, fabrication of high-intense green light emitting diodes (LED) and ternary based high electron mobility transistors (HEMT) are still remains challenging [**4, 5**]. In general, InGaN semiconductors cover a wide range in the solar spectrum between infrared (InN-0.7 eV) to ultraviolet (GaN-3.4 eV). In addition, InGaN has a direct bandgap with high radiation hardness and absorption coefficient (10^5 cm^{-1}) **[1, 6-8].** These properties make InGaN suitable for solar cell applications. However, achieving a homogeneous high indium (In) composition in the InGaN material is not so easy [**9].** Also, the high crystalline quality of InGaN can be attained by reducing the V-pits. The V-pits are commonly observed during the growth of GaN layer and InGaN based quantum wells (QWs) due to the large lattice mismatch between GaN and sapphire substrate. These V-pits have been observed as inverted pyramids along with (1 0 -1 1) faceted sidewalls **[10]**. The reduction in V-pits can be attained when the In composition or InGaN thickness is within its critical value, which improves the interfaces of the InGaN and helps in suppressing the alloy disorders **[11]**. The In incorporation, strain induced bandgap, interfaces, structural quality and annealing effect on the InGaN based structures were already briefly discussed in the literature **[3, 4, 12, 13].** Changda Zheng et.al, introduced the GaN caplayer at same–temperature similar to that of the InGaN QW in order to obtain In-rich InGaN and good interfaces [**14**]. Keller et.al reported that by introducing InGaN/SiN layers between the GaN layers, the dislocation density was reduced [**15**]. The metal organic chemical vapour deposition (MOCVD) growth of InGaN layers at different thickness (20 to 50 nm) on GaN buffer layer was carried out and their corresponding structural, morphological, optical and electrical properties were already reported in the literature [**16**]. In the present study, the growth of GaN layer was

carried out on a thin InGaN interlayer grown at the same temperature as that of GaN to avoid the In decomposition. The effect of InGaN interlayer thickness on the GaN layers were briefly discussed in the present work.

2. Experiments

All the samples were grown on (0 0 0 1) oriented sapphire substrates by horizontal-flow MOCVD system with radio frequency (RF) Heating. Trimethylgallium (TMGa), Triethylgallium (TEGa), Trimethylindium (TMIn), Ammonia (NH_3) were used as Gallium, Indium and nitrogen sources respectively. Hydrogen (H_2) was used as the carrier gas to grow GaN layer. Additionally, nitrogen (N_2) was used as the carrier gas to grow InGaN and GaN caplayer. Prior to high temperature (HT) GaN growth, sapphire substrates were thermally desorbed in hydrogen ambient at 1050ºC for 10 min to remove the surface contamination and adsorbed water molecules. A low-temperature (LT) GaN nucleation layer (NL) was grown with an optimized thickness of about 30 nm. Then, a 2.5 µm thick HT-GaN layer was grown over the nucleation layer, followed by the growth of 5-nm InGaN layer with a V/III ratio of 12970. This sample was named as I. While, sample II contains a 2.5 µm GaN layer, 5-nm InGaN layer and about 50 nm GaN caplayer. Similar to sample II, the thickness of InGaN layer was increased to 10 nm and named as sample III. The experimental details were employed in the present study shown in Table 1. From table 1, the results showcase that the GaN caplayer play a positive effect on the structural, optical and electrical properties. The crystalline qualities of the grown samples were investigated by High-Resolution X-ray Diffractometer (HRXRD-PANalytical X'Pert Pro MRD). Cross-sectional Transmission Electron Microscopy (TEM-Tecnai 20G2, 200keV) was used to verify the layer thickness. Raman measurements (Horiba Jobin Yvon) were performed on InGaN layer using He-Cd laser (325 nm). The surface morphology of the samples were analyzed using Atomic Force

Microscopy (AFM, Park XE-100). The electrical properties of the samples were measured using Hall measurements (ECOPIA, HMS 5000).

Table 1 Experimental details employed for the growth of InGaN Interlayer on GaN layers

<table>
<tr><th rowspan="2">Sample</th><th colspan="2">GaN NL</th><th colspan="2">U-GaN</th><th colspan="5">InGaN</th><th colspan="2">GaN caplayer</th></tr>
<tr><td>T (ºC)</td><td>Time</td><td>T (ºC)</td><td>Time</td><td>T (ºC)</td><td>TMIn µmol/ min</td><td>TEGa µmol/ min</td><td>NH_3 (SLM*)</td><td>Time</td><td>T (ºC)</td><td>Time</td></tr>
<tr><td>I</td><td rowspan="3">500</td><td rowspan="3">6 min</td><td rowspan="3">1020</td><td rowspan="3">90 min</td><td rowspan="3">720</td><td rowspan="3">11</td><td rowspan="3">6.2</td><td rowspan="3">5</td><td>30sec</td><td>-</td><td>-</td></tr>
<tr><td>II</td><td>30 sec</td><td rowspan="2">720</td><td rowspan="2">10 min</td></tr>
<tr><td>III</td><td>60 sec</td></tr>
</table>

*Standard Litres per Minute

3. Results and discussion

3.1. Structural Analysis

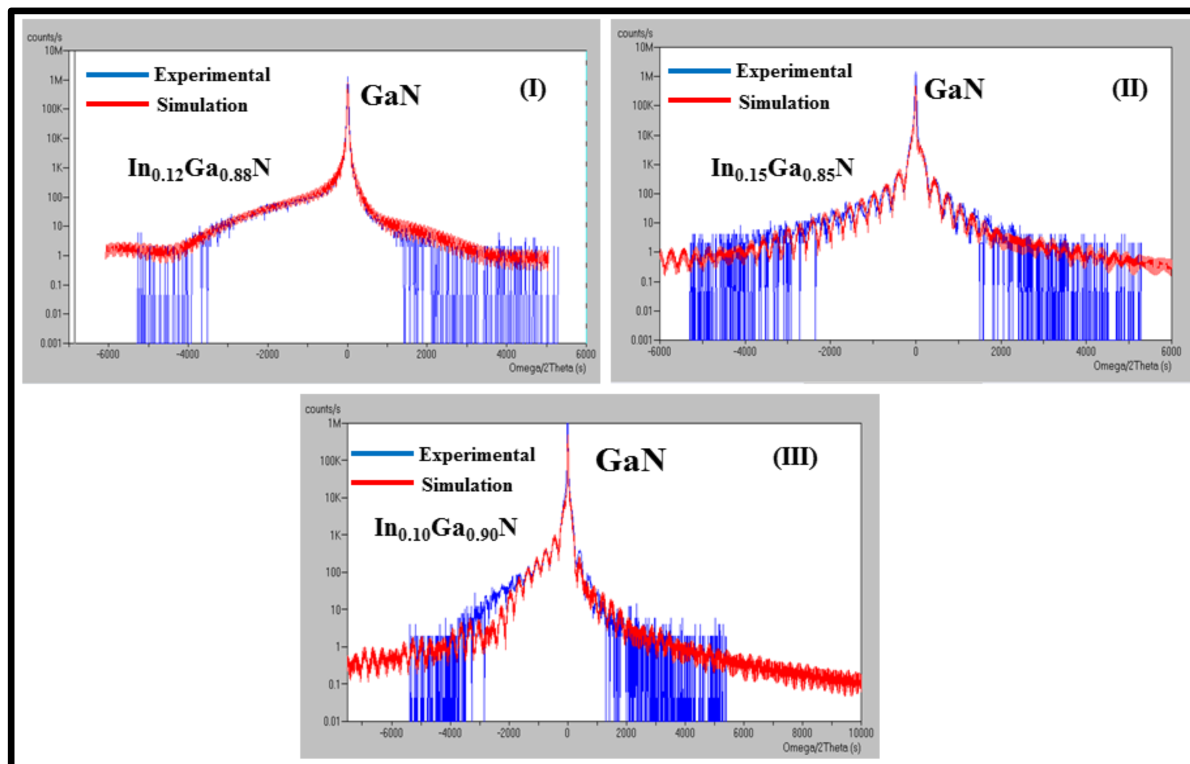

Figure. 1 HRXRD (0 0 0 2) profile for sample (I) InGaN (5 nm)/GaN (II) GaN caplayer/InGaN (5 nm)/GaN (III) GaN caplayer/InGaN (10 nm)/GaN Structures

The ω-2θ scans of (0 0 0 2) diffraction peaks representing sample I, II and III are shown in Figure 1. The experimental data were fitted using epitaxy smooth fit software. The InGaN thickness and In composition of the InGaN interlayer were ascertained from the ω-2θ scan along (0 0 0 2) plane. The diffraction peak of GaN at (0 0 0 2) corresponds to the symmetrical plane of the rocking curve. In sample I, thin InGaN layer was grown on GaN layers. From Figure 1, the peak corresponding to InGaN was broad. Whereas, for samples II and III, satellite peaks are different, due to increasing the InGaN interlayer thickness. The InGaN thickness and In compositions for samples I, II and III were found to be 5 nm, 5 nm and 10 nm, and 12, 15 and 10 % respectively. The thickness of the GaN caplayer was estimated about 50 nm (Figure 1). The full width at half maximum (FWHM) corresponding to (0 0 0 2) of GaN were determined as 367, 356 and 374 arc-sec, FWHM values for (1 0 -1 5) of GaN were 284, 265 and 230 arc-sec for samples I, II and III respectively. The densities of edge (D_{edge}) and screw dislocations (D_{screw}) have been estimated from the HRXRD rocking curve widths of the (1 0 -1 5) and (0 0 0 2) planes for the GaN layers. The threading dislocation (TD) density (TD= D_{edge}+D_{screw}) was calculated from the below equations [**17**],

$$D_{Screw} = \frac{\alpha^2}{4.35|b_{screw}|^2} \qquad D_{edge} = \frac{\beta^2}{4.35|b_{edge}|^2} \tag{1}$$

Where D_{edge} is the edge dislocation density, D_{screw} is the screw dislocation density, α and β are the FWHM value measured from rocking curve diffraction of (0 0 0 2) and (1 0 -1 5) plane, respectively. Here $<b_{edge}>=1/3<11-20>$ is the burger vector of the edge dislocation (a-axis lattice constant) density and $<b_{screw}>=<0001>=C_{0001}$ is the burger vector of the screw dislocation (c-axis lattice constant) density [**18**].The total threading dislocation (TD) density

values of samples I, II and III have been shown in Table 2. The presence of GaN cap layer in sample II reduces the pre-existing screw and edge type dislocation densities in comparison to sample I. It is suggested that the 50 nm thick GaN caplayer can improve the structural homogeneities and/or interface improvement of the In content in the InGaN interlayer on GaN layers through the dissolution of tiny indium rich clusters [**4**]. This increases the In composition in the InGaN layers. In addition, the same was found to get reduced further in sample III. In spite of the reduction in TDs, sample III reveals the composition fluctuations as an effect of intrinsic alloy disordering, resulting in alloy scattering. In general, the alloy scattering can be attributed to the scattering of carriers due to disorder component of the crystal potential [**19**]. Therefore, on basis of the above concept, it emphasizes that, the spatial compositional fluctuation or indium segregation formation in the InGaN layers. As a result, the mobility gets reduced compared to sample II. In addition, similar behavior relating the composition fluctuations have been observed from the PL results [**20**]. Based on the obtained information, sample II possessed better structural quality.

Table 2. Summary of dislocation densities in GaN layers

Samples	Dislocation densities in GaN layers		
	Screw dislocations Density ($10^8 cm^{-2}$)	Edge dislocations Density ($10^8 cm^{-2}$)	TD Density ($10^8 cm^{-2}$)
I	2.70	4.28	6.98
II	2.54	3.69	6.23
III	2.81	2.80	5.61

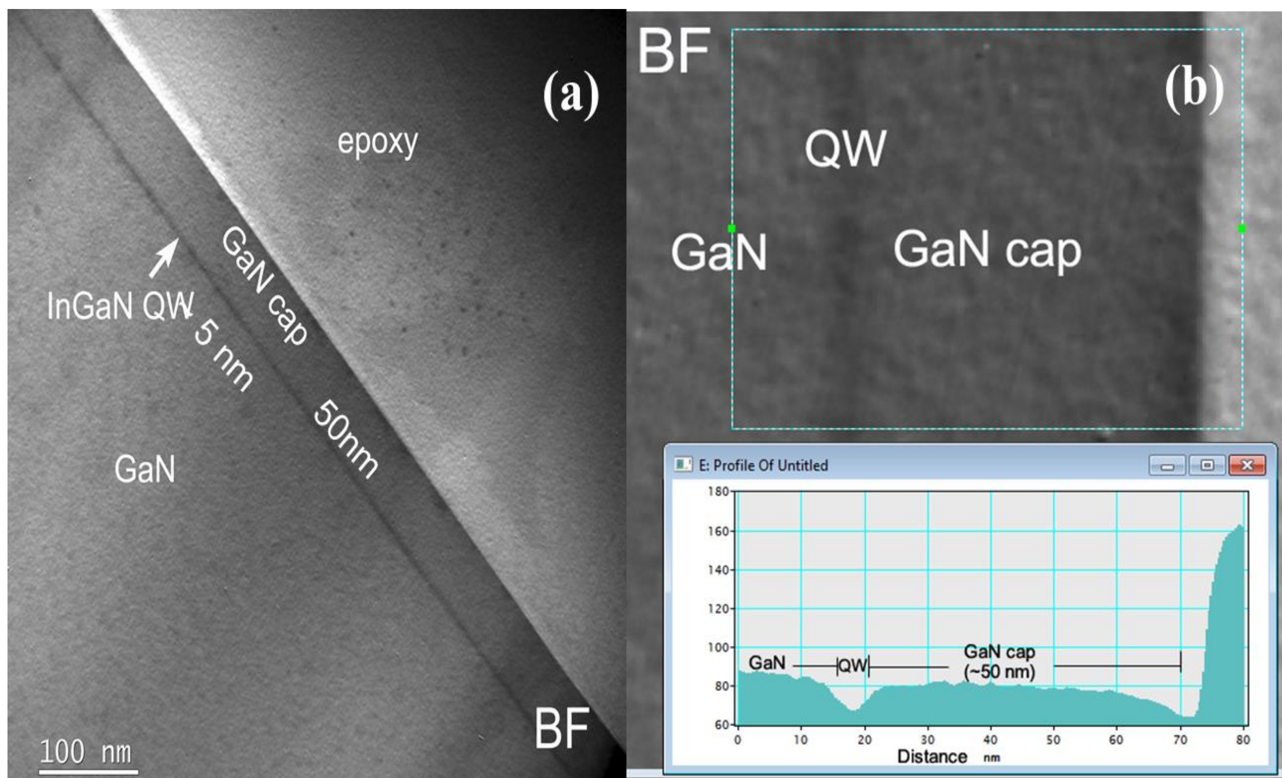

Figure. 2 (a) Cross sectional TEM image (b) Line profile in sample II

Figure 2 (a, b) shows the cross-sectional TEM image of sample II. The interface between the InGaN and GaN caplayer are clearly visible. In the GaN/InGaN/GaN structure, the thickness of InGaN and GaN caplayer were determined as 5 nm and 50 nm, respectively. Since, the thickness of the InGaN interlayer is below its critical thickness, the surface was found predominantly free from V-pits. The growth of GaN caplayer had a positive effect in suppressing and refilling the V-pits [**21**]. The TEM results corroborate the HRXRD results.

The crystalline quality of the InGaN Interlayer on GaN layers were investigated by Raman spectroscopy. Figure. 3 shows the room temperature raman spectra recorded (200-800 cm^{-1}) for the samples I, II and III respectively. These spectra are also compared with the standard GaN (bulk doped) sample as shown in Figure 3. Raman spectra revealed peak at 237 cm^{-1} corresponding to the nanostructures and can be attributed as the zone boundary (ZB) phonon. The peak of 418.7 cm^{-1} corresponds to the sapphire substrate.

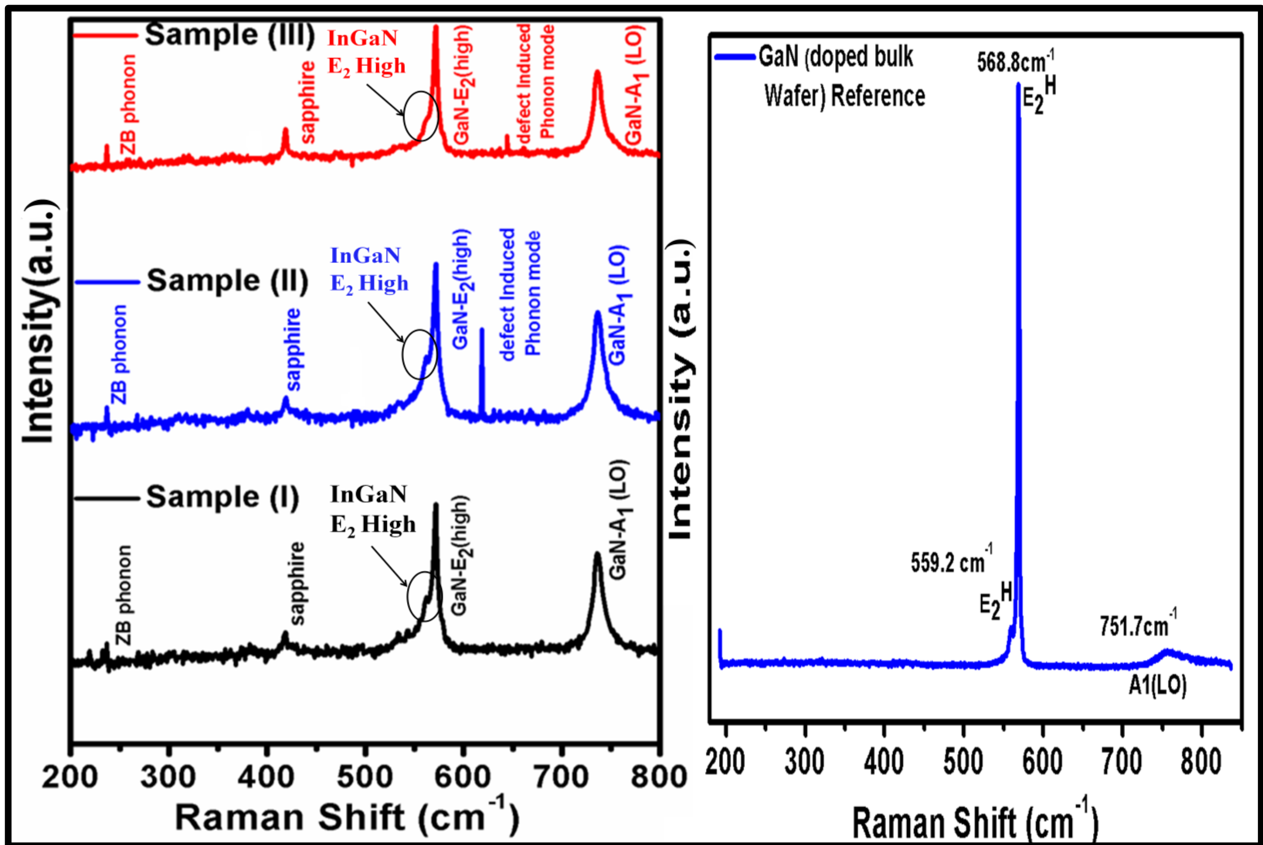

Figure. 3 The room-temperature Raman spectra (samples I-III) of InGaN samples and GaN (doped bulk wafer) reference

The E_2 and A_1 modes of GaN originated from the GaN buffer layer. The spectra displays peaks at 561.78 cm^{-1}, 571.79 cm^{-1} and 735 cm^{-1} corresponds to the wurzite–E_2(high) phonon mode of InGaN, wurzite–E_2(high) phonon mode of GaN and symmetry allowed A_1(LO) phonon mode of GaN layer for the samples I and II respectively. A shift of around ±0.6 cm^{-1} was observed in GaN and InGaN layer for sample III due to the alloy disorder scattering for InGaN Interlayer on the GaN layers. The FWHM of the wurzite–E_2 (high) mode of InGaN layer was found to be~4 cm^{-1} indicating better crystalline quality of InGaN interlayer and also corroborates the HRXRD results. Therefore the growth of single phase InGaN Interlayer on the GaN layers possessed good crystalline quality when compared to literature reports [**22, 23**]. In addition, the samples II and III also represents additional peaks corresponding to the defect induced phonon

mode for InGaN/GaN based structures. This can be attributed to the different spots selected in the sample and the focusing conditions [24].

3.2 Morphological Analysis

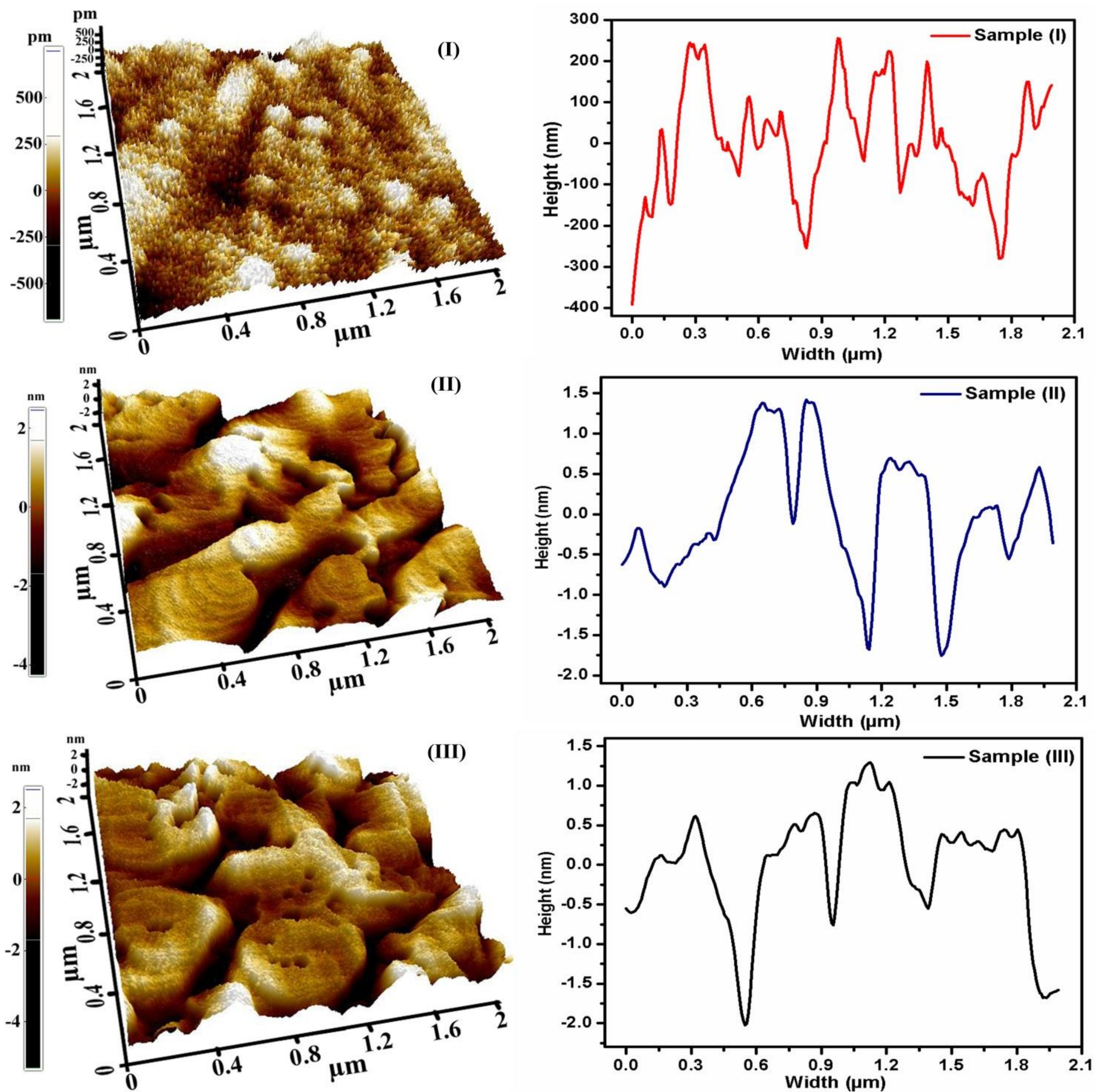

Figure. 4 AFM (2 µm^2) images with line profile of samples I - III

Figure 4 shows the AFM image for samples I, II and III along with line profiles. The RMS roughness of the InGaN/GaN heterostructures were found to be 0.149 nm. From the AFM images of sample I, the surface morphology was observed to be nanometer-sized islands. The width and heights of the islands were found to be ~50 -100 nm and 0.3 – 1 nm respectively. These types of 2D islands tends to relive the strain in the underlying GaN. In samples II and III, RMS roughnesses were estimated as 0.92 nm and 0.86 nm respectively. The variation in the roughness can be attributed to the aggregated nanostructures and the interactions between the neighbouring clusters affecting their shape and size [**25**]. We observed that, widths and height of structures were in the sub-micron range (~ 0.3 - 2 nm). Based on the literature, the growth of low-temperature GaN caplayer has enhanced the nucleation of terrace steps [**26**]. However, in the present study, the GaN caplayer was grown at 720°C which restricts the migration of Ga atoms and results in the formation of helical-like structures. It is worth to note that, the reduction in surface etch pits of sample II is due to the enhanced adatom diffusion during the growth of GaN caplayers and the screw dislocations termination at the InGaN/GaN interface **[27].**

3.3 Electrical Analysis

The Hall measurements of samples I, II and III are shown in table 3. The mobility of InGaN is lower than the GaN layer. This is attributed to more alloy scattering centres being generated when In was added, which in turn reduces mobility [**28**]. Sample I possessed the mobility, bulk and sheet concentration of about 250 cm^2/volt sec, $3.98\times10^{16}/cm^3$ and $1.0\times10^{13}/cm^2$. The presence of GaN caplayer improves the mobility, bulk and sheet concentration of sample II. By further increasing the interlayer thickness, more alloy scattering centres are generated in sample III. This results in mobility limiting due to inhomogeneous In content **[29]**. Comparing the bulk and sheet concentration and resistivity values for all the samples, it was inferred that, the sample I and II exhibits semiconducting behaviour.

Table 3. Electrical properties of InGaN Interlayer on GaN layers

Samples	Mobility cm^2/volt sec	Bulk concentration/ cm^3	Sheet concentration/ cm^2	Resistivity Ohm-cm
I	250	3.98×10^{16}	1.0×10^{13}	0.060
II	316	1.53×10^{17}	3.83×10^{13}	0.012
III	84	6.9×10^{15}	1.73×10^{12}	10.8

4. Conclusions

Growth of GaN layers with InGaN layer on sapphire substrates was carried out using MOCVD. The influence of InGaN interlayer thickness on GaN layer structural, morphological and electrical properties were analyzed using HRXRD, TEM, Raman spectroscopy, AFM and Hall measurements. The thicknesses of InGaN and GaN layers were estimated using HRXRD and was confirmed with the help of cross sectional TEM. It is worth to note that, the InGaN Interlayer was found to reduce the threading dislocations present in the GaN layer. Raman spectroscopy revealed that, the InGaN Interlayer grown on GaN layers exhibit good crystalline quality. From the AFM results, the GaN nanostructures were found to change with underlying InGaN thickness. It confirms that, the addition of 5 nm InGaN as an interlayer between GaN layers significantly improved the electrical properties, and made the surface predominantly free from etch pits. These results help to understand the growth of InGaN which is free from alloy scattering centres. These above discussions indicate that, with InGaN as an interlayer the quality and mobility of GaN layer can be improved further so as to utilize these materials in device based applications.

Acknowledgement

The authors gratefully acknowledge Department of Science and Technology (DST), Government of India (DST/TM/SERI/2K12/71(G)) for funding the research project under SERI. The authors also thank Dr. D.V. Sridhara Rao, Defence Metallurgical Research Laboratory (DMRL), and Hyderabad, India for his constant support in TEM analysis. Author (K.Prabakaran) would like to thank Dr. David Mackenzie, Department of Electronics and Nanoengineering, Aalto University, Finland for his diligent proofreading of this manuscript.

REFERENCES

[1] Fujiyama, Y, Kuwahara, Y, Iwaya, M., Kamiyama, S, Amano, H & Akasaki, I, Phys. Status Solidi C, **7**, 2382 (2010)

[2] Lin, C. F., Chen, K. T., Chen, S. H., Yang, C. C., Huang, W. C., & Hsieh, T. H, J. Cryst. Growth, 370, 97- 100 (2013)

[3] Liu, J., Liang, H., Liu, Y., Xia, X., Huang, H., Tao, P., Sandhu, Q.A., Shen, R., Luo, Y. & Du, G., Mater. Sci. Semicond. Process., 60, 66-70 (2017)

[4] Kaufmann, N. A., Dussaigne, A., Martin, D., Valvin, P., Guillet, T., Gil, B., & Grandjean, N, Semicond. Sci. Technol., 27, 105023 (2012)

[5] Sun, X., Li, D., Song, H., Chen, Y., Jiang, H., Miao, G., & Li, Z. Nanoscale research letters, 7(1), 282. (2012) DOI:10.1186/1556-276X-7-282

[6] Bai, J., Yang, C. C., Athanasiou, M., & Wang, T, Appl. Phys. Lett. , 104, 051129 (2014)

[7] Sundaram, S., Puybaret, R., El Gmili, Y., Li, X., Bonanno, P. L., Pantzas, K., & Ougazzaden, A, J. Appl. Phys., 116, 163105 (2014)

[8] Sanjay, S and Baskar, K., Applied Surface Science, 456, 526-531(2018)

[9] Seo, T. H., Shim, J. P., Chae, S. J., Shin, G., Kim, B. K., Lee, D. S., & Suh, E. K. Appl. Phys. Lett, 102, 031116 (2013)

[10] Lin, F., Xiang, N., Chen, P., Chow, S.Y. and Chua, S.J., J.Appl. Phys., 103(4), 043508 (2008)

[11] Kang, J H, Ebaid, M, Lee, J K & Ryu, S.W., Appl. Phys. A , 121, 765-771 (2015)

[12] Choi, S.K., Jang, J.M., Jung, W.G., Kim, J.Y. and Dai Kim, S., Electronic Materials Letters, 4(2), 67-70 (2008)

[13] Liu, J., Liang, H., Li, B., Liu, Y., Xia, X., Huang, H., Sandhu, Q.A., Shen, R., Luo, Y. and Du, G., RSC Advances, 6(65), 60068-60073 (2016)

[14] Zheng, C., Wang, L., Mo, C., Fang, W and Jiang, F., The Scientific World Journal, 2013, Article ID 538297, 4 pages (2013) DOI :10.1155/2013/538297

[15] Keller, S., Parish, G., Speck, J.S., DenBaars, S.P. and Mishra, U.K., Appl. Phys. Lett., 77(17), 2665-2667 (2000)

[16] Prabakaran, K., Ramesh, R., Jayasakthi, M., Loganathan, R., Surender, S., Pradeep, S., Singh, S. and Baskar, K., Materials today: Proceedings, 4, 12577-12581(2017) DOI : 10.1016/j.matpr.2017.10.064

[17] Lazarev, S., Bauer, S., Forghani, K., Barchuk, M., Scholz, F., & Baumbach, T, J. Cryst. Growth, 370, 51-56 (2013)

[18] Wu, X. H., Brown, L. M., Kapolnek, D., Keller, S., Keller, B., DenBaars, S. P., & Speck, J. S, J. Appl. Phys, 80, 3228-3237 (1996)

[19] Bellotti, E., Bertazzi, F. and Goano, M., J. Appl. Phys, 101(12), 123706 (2007)

[20] Prabakaran, K., Ramesh, R., Jayasakthi, M., Surender, S., Pradeep, S., Balaji, M., Asokan, K. & Baskar, K., Nuclear Instruments and Methods in Physics Research Section B: Beam Interactions with Materials and Atoms, 394, 81-88 (2017) DOI: 10.1016/j.nimb.2016.12.042

[21] Song, T.L., Chua, S.J., Fitzgerald, E.A., Chen, P. and Tripathy, S., Journal of Vacuum Science & Technology A: Vacuum, Surfaces, and Films, 22(2), 287-292 (2004)

[22] Sinha, N., Roul, B., Mukundan, S., Chandan, G., Mohan, L., Jali, V. M., and Krupanidhi, S. B, Mater. Res. Bull. 61, 539-543 (2015)

[23] Correia, M. R., Pereira, S., Pereira, E., Frandon, J., & Alves, E, Appl. Phys. Lett, 83(23), 4761-4763 (2003)

[24] Wu, S.E., Dhara, S., Hsueh, T.H., Lai, Y.F., Wang, C.Y. and Liu, C.P., Journal of Raman Spectroscopy, 40(12), 2044-2049 (2009)

[25] Oliver, R. A., Kappers, M. J., Humphreys, C. J., & Briggs, G. A. D, J. Appl. Phys, 97, 013707(2005)

[26] Miraglia, P. Q., Preble, E. A., Roskowski, A. M., Einfeldt, S., & Davis, R. F, J. Cryst. Growth, 253, 16-25 (2003)

[27] Wu, Z., Shen, X., Xiong, H., Li, Q., Kang, J., Fang, Z., Lin, F., Yang, B., Lin, S., Shen, W. and Zhang, T.Y., Appl. Phys. A, 122, 108 (2016)

[28] Yildiz, A, Dagdelen, F, Acarc, S, Lisesivdin, SB, Kasap, M, Aydogdu, Y & Bosi, M, Acta Phys. Pol. A , 113, 731-739 (2008)

[29] Papadomanolaki, E., Bazioti, C., Kazazis, S.A., Androulidaki, M., Dimitrakopulos, G.P. and Iliopoulos, E., J. Cryst. Growth, 437, 20-25 (2016)